ACS APPLIED MATERIALS & INTERFACES

Research Article

www.acsami.org

Ge Wetting Layer Increases Ohmic Plasmon Losses in Ag Film Due to Segregation

Piotr Wróbel,*,† Tomasz Stefaniuk,*,† Marek Trzcinski,‡ Aleksandra A. Wronkowska,‡ Andrzej Wronkowski,‡ and Tomasz Szoplik†

†University of Warsaw, Faculty of Physics, Pasteura 7 St., 02-093 Warsaw, Poland

‡UTP University of Science and Technology, Institute of Mathematics and Physicsy, Kaliskiego 7 St., 85-789 Bydgoszcz, Poland

Supporting Information

ABSTRACT: We have investigated the influence of the Ge wetting layer on both ohmic and scattering losses of a surface plasmon-polariton (SPP) wave in Ag film deposited on SiO_2 substrate with an e-beam evaporator. Samples were examined by means of atomic force microscopy (AFM), spectroscopic ellipsometry (SE), two-dimensional X-ray diffraction (XRD), X-ray photoelectron spectroscopy (XPS), and microscopic four-point probe (M4PP) sheet resistance measurements. Ag films of 100 nm thickness were deposited at 180 and 295 K directly onto the substrates with or without a Ge interlayer. In AFM scans, we confirm the fact that the commonly used Ge adhesion layer smooths the surface of Ag film and therefore reduces scattering losses of the SPP wave on surface roughness. However, our ellipsometric measurements indicate for the first time that segregation of Ge leads to a considerable increase in ohmic losses connected with a boost of the imaginary part of Ag permittivity in the 500−800 nm spectral range. Moreover, the trend develops over time, as confirmed in a series of measurements performed over an interval of three months. XPS analysis confirms the Ge segregation to the Ag free surface and most probably to grain boundaries. M4PP measurements show that the specific resistivity in Ag films evaporated on a Ge interlayer at 295 K is nearly twice as high as in layers deposited directly on a SiO_2 substrate. The use of an amorphous Al_2O_3 overlayer prevents Ge segregation to free surface.

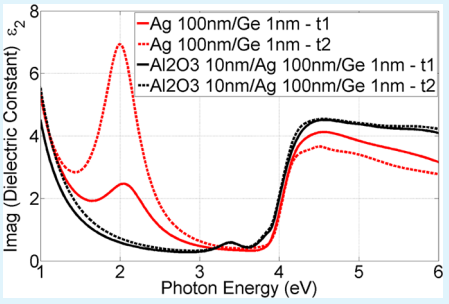

KEYWORDS: *surface plasmon-polariton, scattering losses, ohmic losses, segregation, Ag film, Ge wetting layer*

1. INTRODUCTION

There is currently a great deal of interest for the enhancement of electromagnetic fields connected with resonances of SPP waves on metallic nanostructures.[1−7] This interest lies within a variety of applications, as propagating SPPs are important in surface-enhanced Raman spectroscopy, nonlinear interactions, and transmission through plasmonic metal-dielectric multilayers.[1,3,7] In photovoltaics, the nonradiative decay of localized plasmons on a metal−semiconductor interface leads to the creation of electron−hole pairs in the semiconductor.[2] In spectroscopic biosensors, resonances of localized plasmons are sensitive to refractive index changes induced by biomolecules and measured in either scattered or transmitted light.[4] In near-field optical imaging, the resonance frequency depends not only on the size and shape of the nanoparticle or the nanotip, but also on the permittivity of the surrounding dielectric matrix.[5] The practical value of all the above-mentioned applications is subject to a careful assessment of the SPP energy losses that limit the performance of plasmonic devices.[6]

In the last few decades, the lifetimes and ranges of SPP waves attenuated in thin metal films have been theoretically analyzed and experimentally measured.[8−13] The size of plasmonic circuits is limited by the range of the SPP wave propagating on the dielectric/metal interface; this range decreases due to both ohmic losses arising from the internal structure of the plasmonic material as well as scattering losses from any roughness on the metal surfaces from the fabrication process. Ohmic losses of free electrons in a metal depend both on the type of defects (non-uniformity, grain boundaries, thin-film surfaces) contributing to the electron scattering frequency and on the material temperature and thus cannot be ultimately reduced. Both the uniformity and smoothness of e-beam evaporated metal films can be optimized through the use of an interlayer wetting the substrate[14−20] and proper choice of deposition temperature and rate.[21] Efforts to reduce SPP ohmic and scattering losses should lead to an expansion of the size of plasmonic devices.

In this paper, we discuss the increase of ohmic losses in Ag/Ge/fused silica sandwich due to Ge segregation toward the Ag film surface and probably to metal grain boundaries. To reduce Ge segregation toward the free surface we propose the use of 10-nm-thick Al_2O_3 protective overlayer on top of the Ag/Ge/SiO_2 sandwich. This aluminum oxide overlayer preserves the

Received: October 28, 2014
Accepted: April 14, 2015
Published: April 14, 2015

DOI: 10.1021/acsami.5b01471
ACS Appl. Mater. Interfaces 2015, 7, 8999−9005

smoothness of the silver surface and serves to limit scattering losses.

2. DIFFUSION AND SEGREGATION

At the interface between two solid media atoms, molecules or ions of both materials collide with a temperature-dependent frequency. The result of these random collisions is the diffusion of particles of one medium into the other, i.e., the transport of particles from a region with high concentration to a region of low concentration.[22−25] The diffusion coefficient increases sharply when there are open spaces to be filled in the matrix medium. In such a case the diffusion phenomenon evolves to segregation, which is the separation of admixture atoms in small regions within the matrix medium.

Penetration of atoms, molecules, or ions of one solid medium, such as an elemental semiconductor, into another neighboring one, such as a polycrystalline metal, takes place along high-diffusivity paths and results from segregation into metal grain boundaries, free surfaces, and inhomogeneities.[24] The segregation of germanium on top of Ag films prepared on a Ge(111) substrate was observed for the first time in a study concerning the formation of metal overlayers on semiconductors.[26] Recently, the continuous segregation of Ge at the surface of a growing polycrystalline Ag nanolayer was observed in in situ XPS measurements.[17] It has also been shown that grain-boundary segregation in polycrystalline metals is of significant importance at temperatures lower than 0.6 $T_{melting}$.[24] The melting temperature of thin films deposited on an inert substrate is usually considered to be the temperature at which the film breaks up into droplets.[27] For example, a polycrystalline silver film having a 100 nm thickness deposited onto an inert fused silica substrate has a 1000 K melting temperature, compared with 1235 K for the bulk material.[27] For a 12-nm-thick Ag film on the SiO_2 substrate the metal layer breaks into drops at approximately 500 K.[28] Under the conditions described above, as well as the conditions used within this study, Ge segregation is more important than bulk diffusion.

To understand the segregation mechanism in the transport of Ge atoms in an Ag matrix we performed evaporation onto the samples at two temperatures, at 295 K as well as a much lower temperature of 180 K where the influence of diffusion is reduced. We have previously shown that Ag metal grains are larger in films evaporated at 180 K with respect to Ag layers deposited at 295 K.[21] In the same mass of metal, the area of grain surfaces is larger in fine polycrystalline films than in big grain layers. Under the condition that germanium concentration measurements are made with similar time delay after evaporation, the segregation effect to grain boundaries should be larger in samples evaporated at 295 K.

3. EXPERIMENTAL METHODS

Electron-Beam Physical Vapor Deposition. Thin films were deposited using an electron-beam evaporator (PVD75, Lesker). Single-sided polished fused silica glasses with nominal roughness RMS ≤ 0.3 nm were used as substrates. Before deposition the substrates were cleaned for 30 s with argon ions having 105 eV energy and a 0.2 mA/cm^2 beam density. During the deposition of films the vacuum chamber was kept at room temperature (RT), and the temperature of a custom-made sample holder module was controlled with 1 K accuracy. Germanium layers of 1 nm thickness were evaporated at the rate of 0.5 Å/s at RT. Silver films of 100 nm thickness were deposited at the rate of 10 Å/s at two temperatures, 180 and 295 K. The pressure in the chamber was variable, increasing from 4×10^{-7} Torr to a final value of 2×10^{-6} Torr. We have previously reported the optimum conditions for silver deposition,[20] where we demonstrated that the smoothest Ag surface for 10- and 30-nm-thick layers on a 1 nm Ge wetting layer are evaporated at temperatures ranging from 230 to 350 K. To reduce the effect of germanium segregation to a free surface, a 10 nm Al_2O_3 overlayer was deposited at RT at a rate of 0.5 Å/s. The deposition process for each sample was carried out without breaking the vacuum. Before characterization the samples were kept in ambient conditions in an Ar (6 N) atmosphere.

Atomic Force Microscope Measurements. AFM measurements under tapping mode in air were carried out utilizing an Ntegra NT-MDT microscope equipped with sharp etalon probes with a 10 nm tip curvature radius. The resonant frequency of the probes is equal to 140 kHz, which corresponds to a force constant of 3.5 N/m. The averaged RMS value was measured on several areas of the samples.

Spectroscopic Ellipsometry. The knowledge of exact values of dielectric function is of decisive importance for both modeling and simulations in plasmonics. Ellipsometry and reflectance measurements were made using a rotating analyzer ellipsometer (V-VASE, J.A. Woollam Co., Inc.), and were performed in air in the spectral range from 0.6 to 6.5 eV (193−2200 nm). The change in the polarization state of light reflected from the samples, described in the form of ellipsometric parameters Ψ and Δ, was determined for several angles of incidence in the range $40° \leq \varphi \leq 80°$. Reflectance measurements carried out for transverse electric (TE) and transverse magnetic (TM) polarization of light with electric field vector **E** and magnetic field **H** perpendicular to the plane of incidence, respectively, were performed at $\varphi = 40°$. Optical constants of the samples were calculated from the measured quantities using a regression procedure and the parametrization of optical functions model to match the experimental data.

The refractive index n and the extinction coefficient κ were obtained using a layered box model with either (i) two interfaces, air/Ag and Ag/SiO_2; (ii) three interfaces, air/Ag, Ag/Ge, and Ge/SiO_2; or (iii) four interfaces, air/Al_2O_3, Al_2O_3/Ag, Ag/Ge, and Ge/SiO_2. For the sake of accuracy the model includes an additional top layer composed of silver and air voids to represent the influence of surface roughness on the optical response of the deposited Ag films. The estimation of the thickness of this layer was based on the experimental RMS roughness values acquired from AFM measurements. To parametrize the complex dielectric functions of the Ag layers, the Drude-Lorentz, Tauc-Lorentz, and Gaussian oscillator models were used in the fitting procedure. Optical constants of the thin Ge wetting layer and Al_2O_3 overlayer were taken from the database of commercial software (WVASE 32).

Four-Probe Method. In the four-point probe method, four equally spaced probes are placed in the center of the sample and brought in contact with a metal film.[29] The two outer probes act as the current source and the drop of voltage is measured by the inner ones. The DC resistivity of the samples is determined using a four-point resistivity probe head (Jandell Engineering Ltd.) with Keithley 6221 constant current source and a digital DC nanovoltmeter (Keithley). Current−voltage characteristics were collected at currents lower than 10 mA to avoid the influence of resistance dependence on temperature increase due to ohmic heating. The specific resistivity of a film [$\mu\Omega \cdot$ cm] is a product of experimentally determined resistance of uniform thin film, i.e., the sheet resistance [Ω/sq] and film thickness.

X-ray Photoelectron Spectroscopy. We used a VG-Scienta R3000 hemispherical analyzer with energy resolution set to $\Delta E = 100$ meV. The samples were introduced into an ultrahigh vacuum system with base pressure reaching 2×10^{-10} mbar. Photoemission from the surface was stimulated by a monochromatic Al Kα source ($\hbar\omega$ = 1486.6 eV). XPS measurements were interlaced with Ar ion etching (E = 4 keV, current density 0.175 μA/mm^2, incidence angle 69°). In order to obtain information about the chemical composition of consecutive subsurfaces, an Ar ion beam having a diameter of approximately 1 mm etched a 4×4 mm^2 area. Emitted photoelectrons were collected from a 0.6×0.08 mm^2 region. The atomic concentration of elements was calculated by fitting the strongest peaks to a Gauss-Lorentz line with *CasaXPS* software. The software offers the Monte Carlo method for error analysis. We assess the

DOI: 10.1021/acsami.5b01471
ACS Appl. Mater. Interfaces 2015, 7, 8999−9005

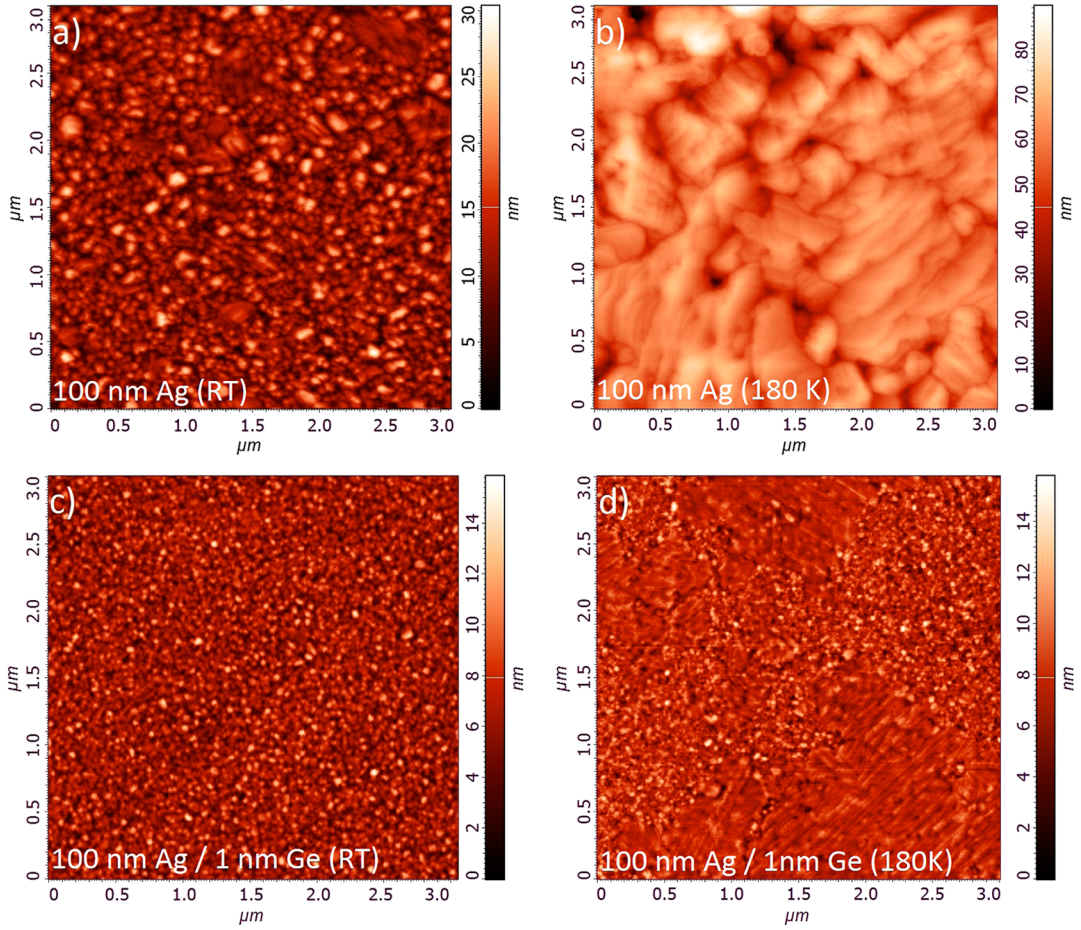

Figure 1. AFM images of a 3 μm × 3 μm area of 100-nm-thick Ag layers deposited on fused silica substrates at 295 K (a, c), at 180 K (b, d), with a germanium wetting layer (c, d), and deposited directly on SiO_2 (a, b).

obtained concentration error on the level of 0.5%. Such small error bars are not visible on the measurement curves.

Two-Dimensional X-ray Diffraction. The structure of thin films was analyzed by wide-angle X-ray diffraction (XRD). The measurements were done using a Bruker GADDS system equipped with a 2D Vantec 2000 detector.

4. RESULTS AND DISCUSSION

Temperature-Dependent Morphology of Ag/SiO_2 and Ag/Ge/SiO_2 Films. The average RMS value measured on silver films deposited directly on fused silica at 295 K (from several uniform areas) was 3.74 ± 0.4 nm, while for those evaporated at 180 K it was 9.28 ± 1.4 nm. The use of a germanium wetting layer has been proposed to reduce the Ag surface roughness, and consequently to limit the SPP wave scattering losses in plasmonic structures.[14] In comparison with the above results, the average RMS value measured on silver films deposited on the Ge interlayer at 295 K was 1.8 ± 0.3 nm. The surface morphology is diverse in Ag films evaporated at 180 K: in disordered areas the average RMS was measured to be 1.8 ± 0.3 nm, while in those with crystalline structures the average RMS was 1.3 ± 0.3 nm.

Figure 1 shows AFM scans of 3 μm × 3 μm areas of 100-nm-thick Ag layers deposited directly onto fused silica substrates (a, b) and with 1 nm thick Ge wetting layer (c, d), where the deposition was performed at both 295 K (a, c) and 180 K (b, d). Samples deposited at these two temperatures have completely different surface morphologies. Evaporation at lower temperature leads to polycrystalline film with much larger grains than those obtained at 295 K. The Ag/SiO_2 sample evaporated at 180 K (Figure 1b) has a grainy structure with large crystal islands reaching 1 μm in size. The Ag/Ge/SiO_2 sample evaporated at 180 K (Figure 1d) is grainy with crystalline structures that are flat (due to adhesion) over a 2 μm distance. The influence of the substrate temperature on the Ag film quality has also been reported elsewhere.[21] The increase of surface roughness with a decrease of temperature does not come from a mismatch of thermal expansion coefficients of the used materials. Rather it is a result from the lower mobility of Ag adatoms that do not assemble in a uniform layer, but their position is instead determined by their point of arrival during the evaporation process. From the point of view of surface smoothness, the optimum silver deposition conditions are achieved at 295 K with a Ge wetting layer.

Increase of Optical Losses in Silver Nanolayers. The optical properties of our samples were investigated by SE and reflectance measurements. The advantage of SE over reflectance measurements is that it has higher sensitivity to surface features, due to direct information on the phase shift (Δ) of the reflected polarized light. The registered optical response depends on both the electron properties of materials and the microstructural properties of each sample. From this point of view the SE measurements offer important, but indirect, information on the dielectric functions, homogeneity, and structural properties of nanostructured systems.

DOI: 10.1021/acsami.5b01471
ACS Appl. Mater. Interfaces 2015, 7, 8999−9005

Figure 2 shows the real $\varepsilon_1 = n^2 - \kappa^2$ (a) and imaginary $\varepsilon_2 = 2n\kappa$ (b) parts of the permittivity of Ag films deposited directly onto fused silica substrate (blue lines) and with a Ge interlayer (red lines) at 295 K and at 180 K (continuous and broken lines, respectively). For reference purposes the experimental data of Ag permittivity from Johnson and Christy[30] (black line) and Palik[31] (dashed black line) are also plotted. The discrepancy between these data in the visible range comes from different fabrication methods of investigated samples. Our measurements show three spectral regions in which the depicted curves have distinctive features. At photon energies close to 4 eV, the onset of interband transitions of electrons can be seen in plots of both real and imaginary parts of permittivity. At higher photon energies all the plots overlap each other. A similar overlap is observed for photon energies below 1.5 eV, where an increase in the imaginary part of the permittivity is connected with the intraband transitions of conduction electrons. In the optical range (2−3 eV) the dielectric function of the 100 nm Ag film deposited directly onto fused silica substrate at 295 K is nearly equal to that given by Johnson and Christy, who measured the real and imaginary parts of the refractive index of Ag films with thickness from 18.5 to 50 nm vacuum-evaporated onto fused silica substrates at room temperature. In the 100 nm Ag film deposited at 180 K the grains are larger with respect to the sample evaporated at 295 K and the mean free path of electrons is longer, which should result in a smaller specific resistivity close to that of bulk silver. Therefore, the imaginary part of the dielectric function of 100 nm Ag film deposited directly onto fused silica substrate at 180 K is close to that of bulk silver given by Palik. For photon energies lower than 2 eV our measured values of ε_2 are higher than those measured by Johnson and Christy and reach those reported by Palik.

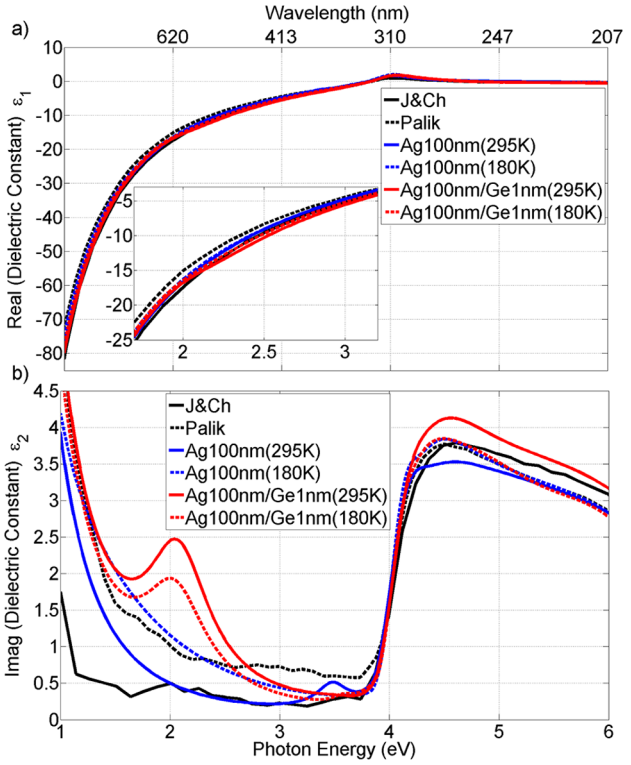

Figure 2. Real (a) and imaginary (b) parts of permittivity of a 100-nm-thick Ag film deposited on fused silica substrate: at 295 K, blue line; at 180 K, blue broken line; with Ge wetting layer at 295 K, red line; and with Ge wetting layer at 180 K, red broken line. Data from Johnson and Christy,[30] black line; and Palik,[31] broken black line; are shown for comparison. Permittivity components are shown as functions of photon energy and corresponding wavelength of light in vacuum.

Weak absorption bands between 3.30 and 3.55 eV refer to the microstructural phenomena that were observed for the permittivity of a 50-nm-thick Ag film evaporated on glass substrate at RT.[32] Svetovoy et al. gave a phenomenological analysis of such additional absorption observed in unannealed Au thin films prepared on different substrates;[33] however, the nature of this band was not explained. Oates et al. postulated that the feature observed at about 3.5 eV in optical spectra of granular Ag films is related to the volume plasmon resonance.[34] This resonance is also known as the Ferrell mode, which only exists in a thin foil and disappears for bulk material.[35] We found that this absorption band is much weaker in the Ag samples deposited at 180 K.

An unexpectedly strong absorption peak appears at 2 eV for samples with a Ge wetting layer, and we connect it with the presence of germanium. The segregation of Ge to both the Ag free surface and grain boundaries leads to a considerable increase of the imaginary part of Ag permittivity in the 500−800 nm spectral range. The evaporation of Ag onto a cooled substrate does not prevent this segregation process, and this absorption peak also appears for samples prepared at 180 K.

To investigate the influence of surface morphology and wetting layer on ohmic losses we measured sheet resistance using the standard four-probe method.[29] Table 1 shows specific resistivity values measured for 100 nm Ag films deposited with and without a Ge wetting layer at 295 and 180 K. The highest value appears for the sample with the Ge underlayer deposited at 295 K. A decrease in the deposition temperature leads to a drop in specific resistivity in both kinds of samples. It can be interpreted that, at low temperatures, the silver film crystallizes to large grains in spite of the presence of Ge. On the contrary, samples deposited at 295 K are smooth, and their grainy structure is suppressed. When grains of the polycrystalline metal layer are smaller than the mean free path of the conduction electrons (equal to 44 nm for bulk Ag[36]), the so-called size effect leads to an increase in specific resistivity due to electron scattering at the grain boundaries. At low temperatures Ag tends to agglomerate in islands with a size close to 1 μm in diameter, which leads to a lower specific resistivity.

Table 1. Specific Resistivity of 100 nm Ag Films Deposited Directly onto Fused Silica Substrates and on 1 nm Ge Wetting Layers

T [K]	sample	ρ [$\mu\Omega\bullet$cm]
295	Ag/SiO_2	2.64 ± 0.03
180	Ag/SiO_2	2.15 ± 0.03
295	$Ag/Ge/SiO_2$	4.65 ± 0.05
180	$Ag/Ge/SiO_2$	2.58 ± 0.03

Germanium Segregation in Silver Films. The increase in optical and ohmic losses in silver films deposited on a Ge wetting layer is investigated using the surface chemical analysis technique XPS. During the procedure successive sublayers of the sample are etched with Ar ions, and the elemental composition of the uncovered surfaces is measured. Figure 3 presents the profiles of atomic concentrations of the main elements as functions of etching time obtained for 100-nm-thick silver film evaporated onto a 1 nm Ge wetting layer and

DOI: 10.1021/acsami.5b01471
ACS Appl. Mater. Interfaces 2015, 7, 8999−9005

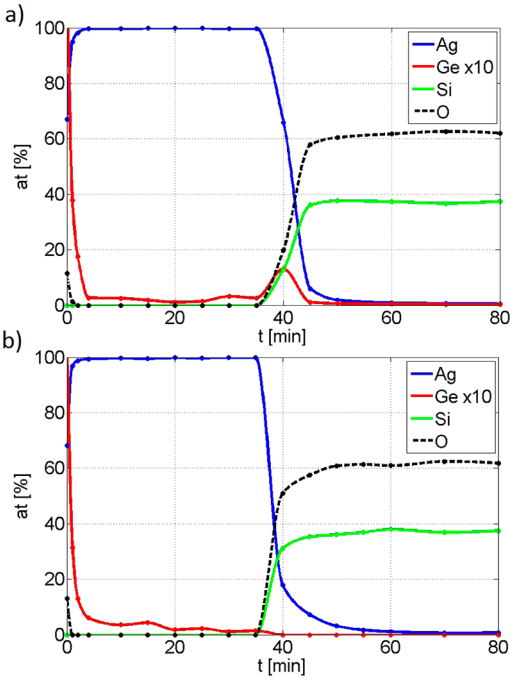

Figure 3. XPS measurements of atomic concentrations of the main elements as a function of Ar-ion etching time with current density 0.175 μA/mm^2 obtained for 100-nm-thick Ag film evaporated at 295 K onto a 1 nm Ge wetting layer on SiO_2 substrate. Profiles taken 2 weeks (a) and 4 weeks (b) after the sample evaporation. The concentration of Ge is multiplied by a factor of 10.

on SiO_2 substrate. The concentration of Ge is multiplied by a factor of 10 in order to preserve the clarity of the plots.

These measurements (Figure 3a) reveal that 14 days after sample evaporation only a fraction of the Ge atoms remain on the fused silica surface under the Ag film, and have diffused into the amorphous substrate. The rest of the Ge atoms segregate into silver grain boundaries and tend to concentrate on the Ag free surface (red line). This is because the grain boundaries of polycrystalline silver samples (and especially the free surface of Ag film) provide sites where Ge solute atoms have lower Gibbs free energy than on the Ge/SiO_2 interface.[24] The segregation of Ge atoms progresses with time: after 28 days the amount of atoms on the Ag/fused silica interface is considerably reduced and the Ge atoms are distributed on both the silver grain boundaries and the Ag free surface (Figure 3b). As a result, Ge atoms located on the silver surface give a momentous contribution to the imaginary part of the Ag permittivity, and thus contribute to the optical losses in the visible spectral range (see Figure 2b).

In Figure 4 we present the time evolution of the imaginary part of the dielectric function of Ag films deposited at 295 K onto fused silica substrate with a Ge interlayer. The red solid line corresponds to ellipsometric measurements performed 24 h after the evaporation (t_1), and the red dashed line presents ε_2 values measured three months later (t_2). The observed evolution of changes of the imaginary part of permittivity at 2 eV is related to germanium segregation into both the Ag grain boundaries and the free surface. The dielectric functions of pure Ag films demonstrate only a slight increase of ε_2 in the free-electron spectral range (energies below 3.5 eV) and a decrease in the interband transitions region. Such behavior is typical for the "pseudo-dielectric" functions determined for metal samples with surfaces deteriorated by the formation of thin oxide layers.

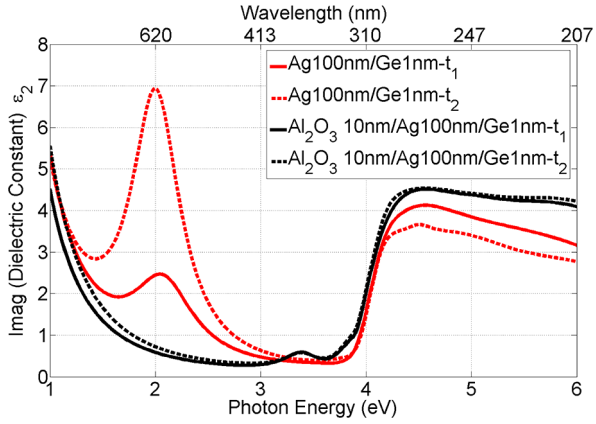

Figure 4. Imaginary part of the permittivity of a 100-nm-thick Ag layer deposited on fused silica substrate with Ge wetting film (red curves), and with an additional Al_2O_3 protective overlayer (black curves). The continuous lines correspond to measurements performed 24 h after the evaporation (t_1), and dashed curves correspond to the same samples characterized again three months later (t_2).

When the silver surface is covered with a 10-nm-thick Al_2O_3 protective overlayer the ellipsometric measurements show that Ge segregation to the Al_2O_3/Ag interface is stopped. The imaginary parts of the dielectric functions for such samples are shown in Figure 4. The black solid line corresponds to ellipsometric measurements taken just after the evaporation process, and the black dashed line corresponds to a sample measured three months later. In both cases there is no trace of strong absorption maxima positioned at 2 eV in their optical response. The only difference is a shift of the ε_2 to higher values in the free-electron part of spectra below 3 eV.

The role of the Al_2O_3 overlayer in Ge segregation is confirmed by XPS surface chemical analysis. Figure 5 presents

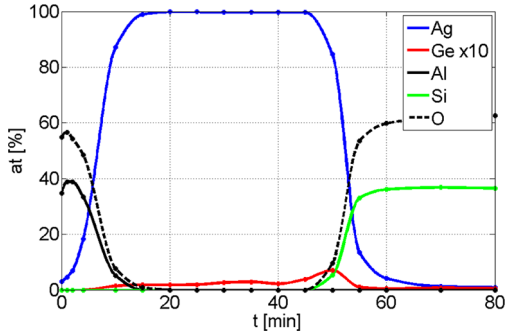

Figure 5. XPS measurements of atomic concentrations of the main elements of the samples as a function of Ar-ion etching time for samples deposited at 295 K with Al_2O_3 protective overlayer. Profile taken 3 weeks after sample evaporation. The concentration of Ge is multiplied by 10.

profiles of atomic concentrations of the main elemental components as functions of etching time measured in a 100-nm-thick Ag film with an Al_2O_3 overlayer and a 1 nm Ge wetting layer on a SiO_2 substrate. It can be seen that, 3 weeks after sample evaporation, the dielectric overlayer leads to a nearly uniform distribution of Ge inside the Ag layer. Thus, the Al_2O_3 overlayer blocks Ge segregation to the Al_2O_3/Ag interface but does not influence Ge segregation to silver grain boundaries. XRD analysis proves that a 10-nm-thick Al_2O_3 film e-beam evaporated at room temperature (RT) on 100 nm Ag

DOI: 10.1021/acsami.5b01471
ACS Appl. Mater. Interfaces 2015, 7, 8999−9005

layer is amorphous. The results from XRD are included in the Supporting Information (SI). In spite of this segregation to the grain boundaries no increase of optical losses was observed, for example, because the skin depth calculated at wavelength 633 nm equals 20.5 nm.

Range of Surface Plasmon-Polariton Wave. Ohmic losses in smooth Ag thin films introduced by the presence of segregated germanium considerably limit the range of the SPP wave. The SPP wave intensity range L is given by the formula

$$L = \frac{1}{2\,\mathrm{Im}(k_{SPP})} = \frac{c}{4\omega}\frac{\varepsilon_1(\varepsilon_1+\varepsilon_d)}{\varepsilon_2\varepsilon_d}\sqrt{\frac{\varepsilon_1+\varepsilon_d}{\varepsilon_1\varepsilon_d}}$$

where ε_1 and ε_2 correspond to real and imaginary parts of the silver permittivity, respectively, and ε_d is the dielectric constant of air.

In Figure 6 we present the ranges of SPP waves propagating on pure Ag films and Ag films with Ge atoms segregated to the surface. Within the visible spectrum, the intensity ranges calculated using our real and imaginary permittivity values of Ag films are close to the data from refs 30 and 31. The ranges of SPP waves propagating on the Ge-covered Ag nanolayer are a few-fold shorter. For example, 24 h after the sample evaporation the intensity range ratio $L_{Ag}/L_{Ag/Ge}$ changes from 1.2 at a wavelength of 400 nm in a vacuum up to 5 at a wavelength of 600 nm.

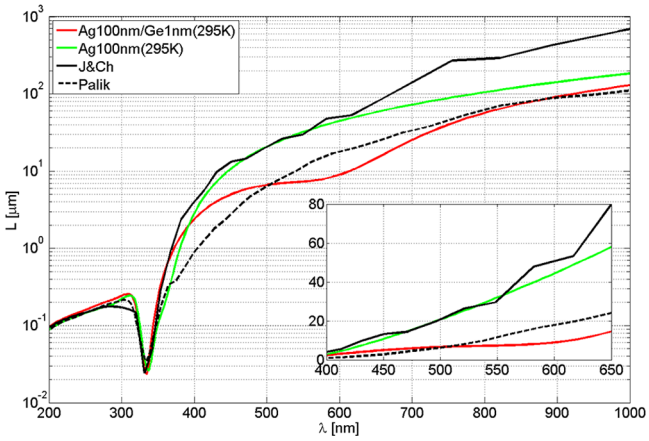

Figure 6. SPP intensity propagation lengths (in logarithmic scale) calculated for pure Ag films and Ag films with Ge atoms segregated to the surface. In the inset, ranges are shown for the visible wavelengths.

5. CONCLUSIONS

We have presented an analysis of ohmic and scattering losses of SPP waves in thin silver films e-beam evaporated on smooth fused silica substrates. Scattering losses due to surface roughness in Ag thin films can be reduced with a Ge wetting interlayer, which reduces island growth due to large adhesion; however, Ge segregates to both the Ag free surface and supposedly grain boundaries, which increases the specific resistivity of Ag films nearly 2-fold in comparison to that of films of the same thickness evaporated directly onto an inert substrate. This increase in losses is more meaningful when we realize that the initial thickness of the evaporated Ge wetting layer is only 1 nm. The Ge segregation develops over time, and the contribution of Ge atoms to optical losses becomes stronger and eventually saturates. Evaporation of Ag onto a cooled substrate does not prevent the segregation process. Here we propose to cover the Ag film with a 10-nm-thick amorphous Al_2O_3 overlayer, which stops the Ge segregation to free surface and preserves the smoothness of the Ag surface.

■ ASSOCIATED CONTENT

Supporting Information

Two-dimensional XRD diffractogram of $Al_2O_3/Ag/SiO_2$ sample recorded within the angular range 2θ = 23.9−48.1° and its one-dimensional cumulated profile. This material is available free of charge via the Internet at http://pubs.acs.org.

■ AUTHOR INFORMATION

Corresponding Authors

*E-mail: piotr.wrobel@igf.fuw.edu.pl.
*E-mail: t.stefaniuk@igf.fuw.edu.pl.

Notes

The authors declare no competing financial interest.

■ ACKNOWLEDGMENTS

This work is supported by the Polish National Center for R&D under the Applied Research Project PBS1/A5/27/2012. The authors thank Professor Ewa Górecka and Dr. Damian Pociecha of the University of Warsaw, Chemistry Department, for the help with XRD analysis.

■ REFERENCES

(1) Kauranen, M.; Zayats, A. V. Nonlinear Plasmonics. *Nat. Photonics* **2012**, *6*, 737−748.
(2) Atwater, H. A.; Polman, A. Plasmonics for Improved Photovoltaic Devices. *Nat. Mater.* **2010**, *9*, 205−213.
(3) Nagpal, P.; Lindquist, N. C.; Oh, S.-H.; Norris, D. J. Ultrasmooth Patterned Metals for Plasmonics and Metamaterials. *Science* **2009**, *325*, 594−597.
(4) Piliarik, M.; Šípová, H.; Kvasnička, P.; Galler, N.; Krenn, J. R.; Homola, J. High-Resolution Biosensor Based on Localized Surface Plasmons. *Opt. Express* **2012**, *20*, 672−680.
(5) Antosiewicz, T. J.; Wróbel, P.; Szoplik, T. Nanofocusing of Radially Polarized Light with Dielectric-Metal-Dielectric Probe. *Opt. Express* **2009**, *17*, 9191−9196.
(6) Boltasseva, A.; Atwater, H. A. Low-Loss Plasmonic Metamaterials. *Science* **2011**, *331*, 290−291.
(7) Kotyński, R.; Stefaniuk, T. Multiscale Analysis of Subwavelength Imaging with Metal-Dielectric Multilayers. *Opt. Lett.* **2010**, *35*, 1133−1135.
(8) Sarid, D. Long-Range Surface-Plasma Waves on Very Thin Metal Films. *Phys. Rev. Lett.* **1981**, *47*, 1927−1930; (erratum). *Phys. Rev. Lett.* **1982**, *48*, 446.
(9) Kuwamura, Y.; Fukui, M.; Tada, O. Experimental Observation of Long-Range Surface Plasmon Polaritons. *J. Phys. Soc. Jpn.* **1983**, *52*, 2350−2355.
(10) Craig, A. E.; Olson, G. A.; Sarid, D. Experimental Observation of the Long-Range Surface Plasmon-Polariton. *Opt. Lett.* **1983**, *8*, 380−382.
(11) Quail, J. C.; Rako, J. G.; Simon, H. J. Long-Range Surface-Plasmon Modes in Silver and Aluminum Films. *Opt. Lett.* **1983**, *8*, 377−379.
(12) Ozbay, E. Plasmonics: Merging Photonics and Electronics at Nanoscale Dimensions. *Science* **2006**, *311*, 189−193.
(13) Berini, P. Long-Range Surface Plasmon Polaritons. *Adv. Opt. Photonics* **2009**, *1*, 484−588.
(14) Logeeswaran, V. J.; Kobayashi, N. P.; Islam, M. S.; Wu, W.; Chaturvedi, P.; Fang, N. X.; Wang, S. Y.; Williams, R. S. Ultrasmooth Silver Thin Films Deposited with a Germanium Nucleation Layer. *Nano Lett.* **2009**, *9*, 178−182.

DOI: 10.1021/acsami.5b01471
ACS Appl. Mater. Interfaces 2015, 7, 8999−9005

(15) Leong, E. S. P.; Liu, Y. J.; Wang, B.; Teng, J. Effect of Surface Morphology on the Optical Properties in Metal-Dielectric-Metal Thin Film Systems. *ACS Appl. Mater. Interfaces* **2011**, *3*, 1148−1153.
(16) Ke, L.; Lai, S. C.; Liu, H.; Peh, C. K. N.; Wang, B.; Teng, J. H. Ultrasmooth Silver Thin Film on PEDOT:PSS Nucleation Layer for Extended Surface Plasmon Propagation. *ACS Appl. Mater. Interfaces* **2012**, *4*, 1247−1253.
(17) Flötotto, D.; Wang, Z. M.; Jeurgens, L. P. H.; Bischoff, E.; Mittemeijer, E. J. Effect of Adatom Surface Diffusivity on Microstructure and Intrinsic Stress Evolutions during Ag Film Growth. *J. Appl. Phys.* **2012**, *112*, 043503.
(18) Formica, N.; Ghosh, D. S.; Carrilero, A.; Chen, T. L.; Simpson, R. E.; Pruneri, V. Ultrastable and Atomically Smooth Ultrathin Silver Films Grown on a Copper Seed Layer. *ACS Appl. Mater. Interfaces* **2013**, *5*, 3048−3053.
(19) Liu, H.; Wang, B.; Leong, E. S. P.; Yang, P.; Zong, Y.; Si, G.; Teng, J.; Maier, S. A. Enhanced Surface Plasmon Resonance on a Smooth Silver Film with a Seed Growth Layer. *ACS Nano* **2010**, *4*, 3139−3146.
(20) Stefaniuk, T.; Wróbel, P.; Trautman, P.; Szoplik, T. Ultrasmooth Metal Nanolayers for Plasmonic Applications: Surface Roughness and Specific Resistivity. *Appl. Opt.* **2014**, *53*, B237−B241.
(21) Stefaniuk, T.; Wróbel, P.; Górecka, E.; Szoplik, T. Optimum Deposition Conditions of Ultrasmooth Silver Nanolayers. *Nanoscale Res. Lett.* **2014**, *9*, 153−161.
(22) Mishin, Y.; Herzig, Chr. Grain Boundary Diffusion: Recent Progress and Future Research. *Mater. Sci. Eng., A* **1999**, *260*, 55−71.
(23) Herzig, C.; Divinski, S. V. Grain Boundary Diffusion in Metals: Recent Developments. *Mater. Trans.* **2003**, *44*, 14−27.
(24) Mehrer, H. *Diffusion in Solids: Fundamentals, Methods, Materials, Diffusion-Controlled Processes*; Springer: Berlin, 2007.
(25) *Handbook of Surface and Interface Analysis Methods for Problem-Solving*, 2nd ed.; Rivière, J. C., Myhra, S., Eds.; CRC Press: Boca Raton, 2009.
(26) Wachs, A. L.; Miller, T.; Chiang, T.-C. Evidence for Germanium Segregation on Thin Films of Ag on Ge(111). *Phys. Rev. B: Condens. Matter Mater. Phys.* **1986**, *33*, 8870−8873.
(27) Gromov, D. G.; Gavrilov, S. A. Heterogeneous Melting in Low-Dimensional Systems and Accompanying Surface Effects. In *Thermodynamics − Physical Chemistry of Aqueous Systems*; Pirajan-Moreno, J. C., Ed.; InTech: New York, 2011.
(28) Kitsyuk, E. P.; Gromov, D. G.; Redichev, E. N.; Sagunova, I. V. Specifics of Low Temperature Melting and Disintegration into Drops of Silver Thin Films. *Prot. Met. Phys. Chem. Surf.* **2012**, *48*, 304−309.
(29) Smits, F. M. Measurement of Sheet Resistivities with the Four-Point Probe. *Bell Syst. Technol. J.* **1958**, *34*, 711−718.
(30) Johnson, P. B.; Christy, R. W. Optical Constants of the Noble Metals. *Phys. Rev. B: Condens. Matter Mater. Phys.* **1972**, *6*, 4370−4379.
(31) *Handbook of Optical Constants of Solids*; Palik, E. D., Ed.; Academic Press: Orlando, 1985.
(32) Wronkowska, A. A.; Wronkowski, A.; Kuklinski, K.; Senski, M.; Skowroński, Ł. Spectroscopic Ellipsometry Study of the Dielectric Response of Au-In and Ag-Sn Thin-Film Couples. *Appl. Surf. Sci.* **2010**, *256*, 4839−4844.
(33) Svetovoy, V. B.; van Zwol, P. J.; Palasantzas, G.; De Hosson, J.; Th, M. Optical Properties of Gold Films and the Casimir Force. *Phys. Rev. B: Condens. Matter Mater. Phys.* **2008**, *77*, 035439(1−12).
(34) Oates, Th. W. H.; Ranjan, M.; Facsko, S.; Arwin, H. Highly Anisotropic Effective Dielectric Function of Silver Nanoparticle Arrays. *Opt. Express* **2011**, *19*, 2014−2027.
(35) Ferrell, R. A. Predicted Radiation of Plasma Oscillations in Metal Films. *Phys. Rev.* **1958**, *111*, 1214−1222.
(36) Kittel, C. *Introduction to Solid State Physics*, 7th ed; John Willey & Sons: New York, 1996.

DOI: 10.1021/acsami.5b01471
ACS Appl. Mater. Interfaces 2015, 7, 8999−9005